Published in final edited form as:

Bioconjug Chem. 2016 July 20; 27(7): 1574–1578. doi:10.1021/acs.bioconjchem.6b00280.

Axial PEGylation of Tin Octabutoxy Naphthalocyanine Extends Blood Circulation for Photoacoustic Vascular Imaging

Haoyuan Huang[†], **Depeng Wang**[†], **Yuzhen Zhang**[‡], **Yang Zhou**[§], **Jumin Geng**[†], **Upendra Chitgupi**[†], **Timothy R. Cook**[‡], **Jun Xia**[†], and **Jonathan F. Lovell**[†,*]

[†]Department of Biomedical Engineering, University at Buffalo, State University of New York, Buffalo, NY, 14260, USA

[‡]Department of Chemistry, University at Buffalo, State University of New York, Buffalo, NY, 14260, USA

[§]College of Chemistry, Chemical Engineering and Materials Science, Collaborative Innovation Center of Functionalized Probes for Chemical Imaging in Universities of Shandong, Key Laboratory of Molecular and Nano Probes, Ministry of Education, Shandong Provincial Key Laboratory of Clean Production of Fine Chemicals, Shandong Normal University, Jinan 250014, P.R. China

Abstract

Attachment of polyethylene glycol (PEG) can prolong blood circulation of biological molecules; a useful trait for a vascular imaging agent. Here, we present a route for modifying octabutoxy naphthalocyanine (ONc) with PEG, via axial conjugation following ONc chelation with Sn(IV) chloride (Sn-ONc). Tin chelation caused ONc absorbance to shift from 860 nm to 930 nm. Hydroxy terminated PEG was treated with sodium and then was axially attached to the tin, generating PEG-Sn-ONc. Unlike ONc or Sn-ONc, PEG-Sn-ONc was soluble in methanol. ONc and PEG-Sn-ONc were dissolved in polysorbate solutions and administered to mice intravenously. PEG-Sn-ONc demonstrated substantially longer blood circulation time than ONc, with a 4 times longer half-life and a nearly 10 times greater area under the curve. PEG-Sn-ONc gave rise to photoacoustic contrast and could be used for non-invasive brain vessel imaging even 24 hours following injection. This work demonstrates that non-metallic naphthalocyanines can be chelated with tin, and be axially modified with PEG for enhanced circulation times for long-term vascular imaging with photoacoustic tomography.

Graphical Abstract

Corresponding Authors: jflovell@buffalo.edu.

ASSOCIATED CONTENT

Supporting Information

NMR, FTIR spectra, cell viability, absorption spectra, and photoacoustic signal analysis.

The authors declare no competing financial interests.

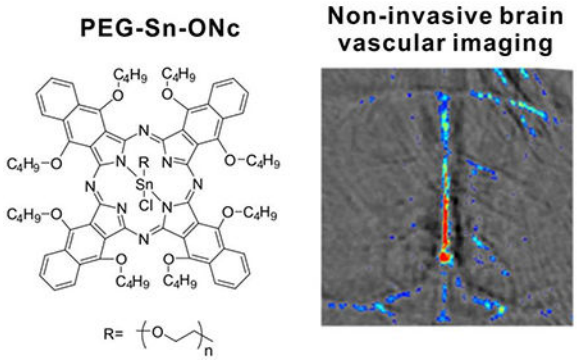

INTRODUCTION

Naphthalocyanine (Ncs) are hydrophobic and aromatic chromophores that exhibit intense absorbance in the near infrared (NIR). Just like related porphyrins and phthalocyanines (Pcs), the two central hydrogen atoms of the tetrapyrrolic macrocycle are active and can be substituted by a wide range of elements (e.g. silicon, zinc, tin, gallium,aluminum, etc.) during the preparation process or via post chelation.[1–4] These central elements can modulate the optical properties of Nc.[5]

Good photostability and high NIR extinction coefficients make Ncs candidates for contrast agents for bioimaging techniques. For example, they have been used for NIR imaging[6], photoacoustic tomography[7,8] and positron emission tomography (PET)[8], making them candidates for multimodal imaging[9]. Ncs generally absorb at longer wavelengths than Pcs, they operate further in the NIR spectrum, where tissue scattering is decreased. However, their extreme hydrophobicity has probably limited their application in these fields. Scientists have attempted to address poor solubility issues by adopting strategies such as modification with of aromatic rings with anionic functional groups.[10,11]

Due to differences in valency, elements chelated in the center of Pcs and Ncs have varying coordination properties. The most common are tetra- (Zn(II))[12,13], penta- (Ga(III) and In (III)) [14–16] or hexa-coordinate (Si(IV) and Sn(IV)) [17–19]. To stabilize the penta- and hexa-coordinate structure, chelation groups, such as chlorides or hydroxyls, are also attached to the axial positions. These axial ligands provide the possibility to modify Pcs and Ncs that do not have other reactive organic groups around the macrocyclic ring through chemical approaches.

Axial silicon Pcs substitutes have been widely studied and applied in both imaging and phototherapeutic applications in vitro and in vivo.[20–23] Polyethylene glycol (PEG) is a hydrophilic and biocompatible polymer chain, and axial conjugation of has been used to improve the hydrophilicity of Pcs.[24] PEGylation has been shown to extend the blood circulation time by reducing reticuloendothelial cell uptake.[25–28] Axial modifications of Ncs for biological applications have not been frequently reported. In one example, Si-Nc was axially modified with hydrophobic oleate moieties to better confer loading into low density lipoproteins.[29] In another example, Si-Nc was modified with small hydrophilic PEG chains (molecular weight 1900 Da) for aqueous intravenous administration to rodents, although

little dye remained in serum by 24 hours.[30] To the best of our knowledge there have not yet been reports involving axial modifications of Sn(IV) Ncs for biomedical imaging applications.

While tetrapyrroles can be conjugated to polymers through a variety of convenient routes such as amidation[31], the axial route provides an elegant and practically intrinsic handle for conjugation. Here, we adopt a post-chelation approach involving insertion of Sn into the pre-formed ONc macrocycle to generate Sn(IV) octabutoxy-naphthalocyanine (Sn-ONc). We then demonstrate an axial PEGylation strategy that extends circulation time for long-term vasculature imaging with photoacoustic computed tomography (PACT).

PACT is an emerging diagnostic technique provides the potential of monitoring contrast in biological tissues with high contrast and high depth.[32–35] PACT can penetrate much deeper into living bodies than other optical techniques, and detect the biological objectives range from organelles to organs, such as kidney [36], brain [37] and tumors [38]. Phosphorous Pc has been used as a PACT contrast agent and was detected through an entire 5 cm human arm.[39] Octabutoxy-naphthalocyanine (ONc) encapsulated into Pluronic micelles has been used for a variety of such applications.[8,40,41] It is known that after introducing Sn (IV) to the center, Sn-ONc possesses a longer absorbance close to 930 nm, compared to its original 863 nm.[4]

RESULTS AND DISCUSSION

The ONc tin chelation and axial PEGylation process is shown in Figure 1A. $SnCl_2$ chelation to ONc followed the method reported by Bae and coworkers.[4] ONc was reacted with $SnCl_2$ in anhydrous DMF for 4h and then was purified with a size exclusive column to yield Sn-ONc. Without further modification, axial chloride of Sn-ONc was replaced by reaction with silver hexafluorophosphate in toluene overnight. PEG-10K (with one terminal hydroxyl group) was reacted with NaH in toluene anhydrous to generate Na-PEG-10K. Na-PEG-10K was combined with the hexafluorophosphate Sn-ONc solution and further reacted for 48h to obtain the final PEGylated compound, PEG-Sn-ONc. The NMR data of all of the compounds are shown as Figure S1 and Figure S2. IR data are shown in Figure S3.

With gel permeation chromatography, the product demonstrated a similar but slightly earlier elution time as PEG-10K alone, but a much later elution time than PEG-20K (Figure 1B). This indicates there was only one PEG-10K chain successfully conjugated to the axial position. Because of the long PEG chain used, steric hindrance from the PEG may have blocked reactive groups on one side of the dye. PEG-Sn-ONc had a similar absorbance spectrum as Sn-ONc, demonstrating that PEGylation did not alter electronic configurations of the Nc (Figure 1C). ONc, Sn-ONc and PEG-Sn-ONc were adjusted to the same molar concentration and were dissolved in methanol. Following centrifugation to remove aggregates, the supernatants were diluted 100 times to test their absorbance. As shown in Figure 1D, PEG-Sn-ONc demonstrated high methanol solubility compared to the other two compounds, showing that PEG addition improves solubility in a polar solvent.

The cytotoxicity of PEG-Sn-ONc was examined in vitro in U-87 cancer cells (Figure S4). It generally demonstrated similar cytotoxicity as the commonly used NIR dye methylene blue.

For in vivo studies, PEG-Sn-ONc or ONc was dissolved in polysorbate-20 (TWEEN 20) and intravenously administered to mice. After injection of 6 optical densities (O.D.) of sample (200 μL, with a NIR absorbance of 30 for a 1 cm pathlength cuvette after considering the dilution factor), PEG-Sn-ONc exhibited a much longer blood circulation time than ONc, as shown in Table 1. The area under the curve parameter was nearly 10 times greater for PEG-Sn-ONc than ONc (Figure 2A). Biodistribution was assessed using NIR optical absorption measurements of homogenized tissues. At the 24 hour time point, a large proportion of PEG-Sn-ONc, but very little ONc, remained in blood (Figure 2B). ONc was taken up mostly in the liver and spleen. This is consistent with the paradigm that PEGylation can induce evasion of macrophages in the reticular endothelial system, which is largely represented by the liver and spleen.[42] Similar result have been observed in other materials which were coated with longer chain PEGs. Lipka et al. found that gold nanoparticles coated with PEG-10K demonstrated longer blood circulation time with lower amounts of liver and spleen uptake relative to those coated with PEG-750.[43] There are also several other parameters that could affect macrophage uptake including the conformation of the biomaterials.[44]

The longer blood circulation time provides the possibility for long-term blood vessels monitoring. Because of its NIR absorbance, PEG-Sn-ONc was used as contrast agent for long-term blood vessels imaging by PACT. 6 optical densities (O.D.) of ONc or PEG-Sn-ONc were injected into mice and the signals of brain vessels were monitored immediately and 24h post injection. Photoacoustic imaging wavelengths were selected on the basis of the peak absorption of each dye in TWEEN 20 (Figure S5). Mice had fully intact skulls during the procedure. As shown in Figure 3, PEG-Sn-ONc illustrated a clearer photoacoustic map of the brain vessels than ONc immediately after the injection. 24h later, the PEGylated ONc still demonstrated strong photoacoustic signals while the signals from ONc group were low, and were almost the same as the untreated control group. The overall photoacoustic intensities of these three groups were quantified and are shown in Figure S6. By 24 hours, the non-PEGylated ONc group had returned to the same photoacoustic intensity of the control mice, whereas the PEG-Sn-ONc group photoacoustic signal remained elevated.

In summary, the chelation of Sn (IV) to the center of ONc shifts its absorbance from 860 nm to 930 nm. Axial PEGylation was then performed with the Sn-ONc macrocycle intact and with unchanged NIR absorbance. The PEG chain provided improved solubility in polar solvents. After injection into mice, PEG-Sn-ONc exhibited longer blood circulation than ONc. Mice showed strong photoacoustic signals 24h post injection to enable vascular brain imaging. In the future, other functional groups could be used to modify the axial position of these Ncs to achieve modulated biological properties.

EXPERIMENTAL SECTION

Materials:

5,9,14,18,23,27,32,36-Octabutoxy-2,3-naphthalocyanine (ONc) was from HPPE Co., tin dichloride was from Alfa Aesar, PEG-10K, PEG 20-K and silver hexafluorophosphate were from Sigma Aldrich, TWEEN 20 was from Amresco, Biobeads SX-1 were from Bio-Rad Laboratories, XTT was from Biotium. ICR mice were ordered from Harlan Laboratories.

Post chelation of tin dichloride into ONc.

58 mg (0.045 mmol) ONc was mixed with 300 mg (1.33 mmol) $SnCl_2$ in anhydrous DMF and refluxed for 4h. DMF was removed by rotary evaporator. The product was obtained by purification with Biobeads SX-1 size exclusive column in toluene. 40.2 mg of product was obtained (0.027 mmol) (60.5% yield). ^{1}H NMR (500 MHz, benzene-d6): δ=9.14 (m, 8H, 1,4-Nc H); 7.67 (m, 8H, 2,3-Nc H); 5.25 (t, 16H, Bu-α-CH2); 2.24 (m, 16H,Bu-β-CH2); 1.62 (m, 16H, Bu-γ-CH2); 1.01 (t, 24H, Bu-CH3). MS (Maldi-TOF): m/z=1478.56 [M+] (calculated 1479).

Synthesis of PEG-Sn-ONc.

The axial chloride of $SnCl_2$ONc (100 mg, 0.068 mmol) was removed using silver hexafluorophosphate (170.94mg, 0.68mmol) in toluene at 60 °C overnight. In the meantime, polyethlyene glycol-10,000 (PEG-10K) (2,040 mg, 0.204 mmol) was refluxed with NaH (60% dispersion, 8.16 mg, 0.204 mmol) in anhydrous toluene for 3h. After the Na-PEG-10K toluene solution cooled to 60 °C, it was transferred to the $SnCl_2$ONc-hexafluorophosphate toluene solution, and refluxed at 115 °C for 48h. Toluene was removed by rotary evaporation, and then the product was washed with ethyl ether and methanol to precipitate out unincorporated PEG-10K and $SnCl_2$ONc. The product was further purified by Biobeads SX-1 size exclusion column in toluene. 77.4 mg of product was obtained (10% yield). ^{1}H NMR (500 MHz, benzene-d6): δ=8.39 (m, 8H, 1,4-Nc H); 7.29 (m, 8H, 2,3-Nc H); 4.47 (t, 16H, Bu-α-CH2); 3.48 (m, 938H, PEG-CH2); 1.78 (m, 16H, Bu-β-CH2); 1.47 (m, 16H, Bu-γ-CH2); 0.88 (t, 24H, Bu-CH3).

Cell Viability.

Human glioblastoma (U87) cells were cultured in Dulbecco's modified Eagle's medium supplemented with 10% fetal bovine serum (FBS) and 1% penicillin-streptomycin and were maintained at 37 °C with 5% CO2. Cells were seeded in a 96-well plate at a concentration of 2×10^4 cells/ well 24 hours before the addition of polymer samples. PEG-ONc sample was added to wells containing DMEM with serum to achieve a final concentration as indicated in the figure. Sample containing media was removed 24 hours later and the wells were washed with PBS before adding fresh media with FBS. To perform XTT assay, media was aspirated out and cells were washed with 100uL of PBS gently. 100uL of PBS containing XTT (50 μg/mL) and of PMS (N-methyl dibenzopyrazine methyl sulfate) (60 μg/mL) was added to each well. Plate was read 2 hours after XTT treatment at 450 nm and 630 nm (background). Cell viability was calculated as the ratio of treated cells to untreated cells after subtracting blank values from both sets. All measurements were made in triplicates.

In vivo studies.

Animal studies were carried out in accordance with the University at Buffalo IACUC. 10 mg of PEG-Sn-ONc was dissolved in 100 uL TWEEN 20 and the mixture was sonicated and centrifuged at 14000 rpm for 15 min to remove aggregates. The solution was diluted with water to obtain a NIR absorbance of 30, the solution was centrifuged again to remove any aggregates and the absorbance of the solution was confirmed. Female ICR mice were injected with 200 μL solution (for NIR O.D.=6). Blood samples were collected at 1h, 2h, 4h,

6h, 8h, 12h and 24h post injection. Serum was obtained following centrifugation for 15 min at 2000 rpm and was diluted in water to measure the NIR absorbance. PKSolver software was used to determine pharmacokinetic parameters. Organs including heart, liver, spleen, lung, kidney and blood were collected for biodistribution. Organ pieces were mixed with 500 μL nuclear lysis buffer [0.25 mol/L sucrose, 5 mmol/L TriseHCl, 1 mmol/L $MgSO_4$,1 mmol/L $CaCl_2$ (pH 7.6)] and were homogenized with a steel bead-based Bullet Blender homogenizer according to manufacturer recommendation. Supernatants were centrifuged and absorbance was measured. Absorbance was tested and compared to the original absorbance of administrated solution to calculate the biodistribution. For the mice administrated with ONc, the same organs were collected and ONc distribution was determined using previously published methods involving dichloromethane extraction.[8]

PA imaging.—An Nd:YAG pumped OPO laser (SureliteTM OPO Plus, Continuum) was chosen as the excitation light source. The laser beam was routed to the mouse brain through a 1.2 cm diameter fiber bundle. The maximum light intensity at the scalp was around 14 mJ/cm^2, which was far below the American National Standards Institute (ANSI) safety limit of 50 mJ/cm^2 for 900 and 60 mJ/cm^2 for 940 nm. The photoacoustic signal was detected with a customized ¾ ring transducer array with 128 elements and 5 MHz central frequency. The radius of the ring array was 40 mm and each element formed an elevation focus at 35 mm. Thus elevation resolution and receiving sensitivity are relatively uniform at the central 10 mm radius region. The received PA signals were amplified (by 54 dB) and digitized by a 128-channel ultrasound data acquisition system (Vantage, Verasonics). The raw channel data was reconstructed and displayed in real-time using the universal back-projection algorithm.[45] Two ICR mice were imaged immediately and 24 h after injecting 6. O.D. ONc or PEG-Sn-ONc, respectively. A control mouse without injection was also imaged for comparison.

Supplementary Material

Refer to Web version on PubMed Central for supplementary material.

ACKNOWLEDGMENTS

This work was made possible in part by funding from the National Institutes of Health (Grant Nos. 1R01CA169365 and DP5OD017898) and the National Natural Science Foundation of China (No. 21401118).

REFERENCES

(1). Ford WE; Rodgers MAJ; Schechtman LA; Sounik JR; Rihter BD; Kenney ME Synthesis and photochemical properties of aluminum, gallium, silicon, and tin naphthalocyanines. Inorg. Chem 1992, 31 (16), 3371.

(2). Wheeler BL; Nagasubramanian G; Bard AJ; Schechtman LA; Kenney ME A silicon phthalocyanine and a silicon naphthalocyanine: synthesis, electrochemistry, and electrogenerated chemiluminescence. J. Am. Chem. Soc 1984, 106 (24), 7404.

(3). Yu L; Zhou X; Yin Y; Liu Y; Li R; Peng T Highly Asymmetric Tribenzonaphtho-Condensed Porphyrazinatozinc Complex: An Efficient Near-Infrared Sensitizer for Dye-Sensitized Solar Cells. ChemPlusChem 2012, 77 (11), 1022.

(4). Bae C; Kwag G; Kenney ME Synthesis and characterization of near-infrared absorption tin octabutoxy naphthalocyanines. Polyhedron 2007, 26 (12), 2810.

(5). Williams RJP The Properties Of Metalloporphyrins. Chem. Rev 1956, 56 (2), 299.

(6). Xiong L; Shuhendler AJ; Rao J Self-luminescing BRET-FRET near-infrared dots for in vivo lymph-node mapping and tumour imaging. Nat. Commun 2012, 3, 1193. [PubMed: 23149738]

(7). Aoki H; Nojiri M; Mukai R; Ito S Near-infrared absorbing polymer nano-particle as a sensitive contrast agent for photo-acoustic imaging. Nanoscale 2015, 7 (1), 337. [PubMed: 25407911]

(8). Zhang Y; Jeon M; Rich LJ; Hong H; Geng J; Zhang Y; Shi S; Barnhart TE; Alexandridis P; Huizinga JD et al. Non-invasive multimodal functional imaging of the intestine with frozen micellar naphthalocyanines. Nat. Nanotechnol 2014, 9 (8), 631. [PubMed: 24997526]

(9). Rieffel J; Chitgupi U; Lovell JF Recent Advances in Higher-Order, Multimodal, Biomedical Imaging Agents. Small 2015, 11 (35), 4445. [PubMed: 26185099]

(10). Luan L; Chen J; Ding L; Wang J; Cheng X; Ren Q; Liu W Tetrabrominated Naphthalocyaninatozinc Complex with Terminal Carboxylate Functionalities. Chem. Lett 2012, 41 (9), 1012.

(11). Spikes JD; van Lier JE; Bommer JC A comparison of the photoproperties of zinc phthalocyanine and zinc naphthalocyanine tetrasulfonates: model sensitizers for the photodynamic therapy of tumors. J. Photochem. Photobiol., A: Chem 1995, 91 (3), 193.

(12). Hanack M Glycosylated metal phthalocyanines. Molecules 2015, 20 (11), 20173. [PubMed: 26569201]

(13). Luan L; Ding L; Zhang W; Shi J; Yu X; Liu W A naphthalocyanine based near-infrared photosensitizer: Synthesis and in vitro photodynamic activities. Bioorg. Med. Chem. Lett 2013, 23 (13), 3775. [PubMed: 23721806]

(14). Schneider T; Heckmann H; Barthel M; Hanack M Synthesis and Characterization of Soluble Chloro-and Aryl (naphthalocyaninato) indium (III) Complexes and Their Precursors. Eur. J. Org. Chem 2001, 2001 (16), 3055.

(15). Calvete M; Yang GY; Hanack M Porphyrins and phthalocyanines as materials for optical limiting. Synt. Met 2004, 141 (3), 231.

(16). Chen Y; Hanack M; Araki Y; Ito O Axially modified gallium phthalocyanines and naphthalocyanines for optical limiting. Chem. Soc. Rev 2005, 34 (6), 517. [PubMed: 16137164]

(17). Hayashida S; Hayashi N Effect of axial substituents on the aggregate of silicon naphthalocyanine in the vacuum deposited thin films. Chem. Lett 1990, (11), 2137.

(18). Tai S; Hayashida S; Hayashi N Photo-induced electron-transfer reaction of naphthalocyanine. J. Chem. Soc., Perkin Trans 1991, (2), 1637.

(19). Jakubikova E; Campbell IH; Martin RL Effects of Peripheral and Axial Substitutions on Electronic Transitions of Tin Naphthalocyanines. J. Phys. Chem. A 2011, 115 (33), 9265. [PubMed: 21800923]

(20). Lau JTF; Lo P-C; Jiang X-J; Wang Q; Ng DKP A Dual Activatable Photosensitizer toward Targeted Photodynamic Therapy. J. Med. Chem 2014, 57 (10), 4088. [PubMed: 24793456]

(21). Zhu Y-J; Huang J-D; Jiang X-J; Sun J-C Novel silicon phthalocyanines axially modified by morpholine: Synthesis, complexation with serum protein and in vitro photodynamic activity. Inorg. Chem. Commun 2006, 9 (5), 473.

(22). Bio M; Rajaputra P; Nkepang G; You Y Far-Red Light Activatable, Multifunctional Prodrug for Fluorescence Optical Imaging and Combinational Treatment. J. Med. Chem 2014, 57 (8), 3401. [PubMed: 24694092]

(23). Zhao Z; Gambari R; Lee KK-H; Kok SH-L; Wong RS-M; Lau F-Y; Tang JC-O; Lam K-H; Cheng C-H; Hau DKPet al. In vivo antitumour activity of amphiphilic silicon(IV) phthalocyanine with axially ligated rhodamine B. Bioorg. Med. Chem. Lett 2013, 23 (8), 2373. [PubMed: 23473678]

(24). Huang J-D; Wang S; Lo P-C; Fong W-P; Ko W-H; Ng DK Halogenated silicon (IV) phthalocyanines with axial poly (ethylene glycol) chains. Synthesis, spectroscopic properties, complexation with bovine serum albumin and in vitro photodynamic activities. New J. Chem 2004, 28 (3), 348.

(25). Daou TJ; Li L; Reiss P; Josserand V; Texier I Effect of Poly(ethylene glycol) Length on the in Vivo Behavior of Coated Quantum Dots. Langmuir 2009, 25 (5), 3040. [PubMed: 19437711]

(26). Peng C; Zheng L; Chen Q; Shen M; Guo R; Wang H; Cao X; Zhang G; Shi X PEGylated dendrimer-entrapped gold nanoparticles for in vivo blood pool and tumor imaging by computed tomography. Biomaterials 2012, 33 (4), 1107. [PubMed: 22061490]

(27). Wen S; Zhao Q; An X; Zhu J; Hou W; Li K; Huang Y; Shen M; Zhu W; Shi X Multifunctional PEGylated Multiwalled Carbon Nanotubes for Enhanced Blood Pool and Tumor MR Imaging. Adv. Healthc. Mater 2014, 3 (10), 1568. [PubMed: 24665035]

(28). Zhou B; Zheng L; Peng C; Li D; Li J; Wen S; Shen M; Zhang G; Shi X Synthesis and Characterization of PEGylated Polyethylenimine-Entrapped Gold Nanoparticles for Blood Pool and Tumor CT Imaging. ACS Appl. Mater. Interfaces 2014, 6 (19), 17190. [PubMed: 25208617]

(29). Song L; Li H; Sunar U; Chen J; Corbin I; Yodh AG; Zheng G Naphthalocyanine-reconstituted LDL nanoparticles for in vivo cancer imaging and treatment. Int. J. Nanomedicine 2007, 2 (4), 767. [PubMed: 18203443]

(30). Bellemo C; Jori G; Rihter BD; Kenney ME; Rodgers MA Si(IV)-naphthalocyanine: modulation of its pharmacokinetic properties through the use of hydrophilic axial ligands. Cancer letters 1992, 65 (2), 145. [PubMed: 1511419]

(31). Chitgupi U; Zhang Y; Lo CY; Shao S; Song W; Geng J; Neelamegham S; Lovell JF Sulfonated Polyethylenimine for Photosensitizer Conjugation and Targeting. Bioconjugate Chem 2015, 26 (8), 1633.

(32). Wang LV; Hu S Photoacoustic Tomography: In Vivo Imaging from Organelles to Organs. Science 2012, 335 (6075), 1458. [PubMed: 22442475]

(33). Xu M; Wang LV Photoacoustic imaging in biomedicine. Rev. Sci. Instrum 2006, 77 (4), 041101.

(34). Kim C; Favazza C; Wang LV In Vivo Photoacoustic Tomography of Chemicals: High-Resolution Functional and Molecular Optical Imaging at New Depths. Chem. Rev 2010, 110 (5), 2756. [PubMed: 20210338]

(35). Xia J; Kim C; Lovell JF Opportunities for Photoacoustic-Guided Drug Delivery. Curr. Drug Targets 2015, 16 (6), 571. [PubMed: 26148989]

(36). Song KH; Wang LV Noninvasive photoacoustic imaging of the thoracic cavity and the kidney in small and large animals. Med. Phys 2008, 35 (10), 4524. [PubMed: 18975699]

(37). Wang X; Pang Y; Ku G; Xie X; Stoica G; Wang LV Noninvasive laser-induced photoacoustic tomography for structural and functional in vivo imaging of the brain. Nat. Biotechnol 2003, 21 (7), 803. [PubMed: 12808463]

(38). Mehrmohammadi M; Yoon SJ; Yeager D; Emelianov SY Photoacoustic Imaging for Cancer Detection and Staging. Curr. Mol. Imaging 2013, 2 (1), 89. [PubMed: 24032095]

(39). Zhou Y; Wang D; Zhang Y; Chitgupi U; Geng J; Wang Y; Zhang Y; Cook TR; Xia J; Lovell JF A Phosphorus Phthalocyanine Formulation with Intense Absorbance at 1000 nm for Deep Optical Imaging. Theranostics 2016, 6 (5), 688. [PubMed: 27022416]

(40). Lee C; Kim J; Zhang Y; Jeon M; Liu C; Song L; Lovell JF; Kim C Dual-color photoacoustic lymph node imaging using nanoformulated naphthalocyanines. Biomaterials 2015, 73, 142. [PubMed: 26408999]

(41). Zhang Y; Song W; Geng J; Chitgupi U; Unsal H; Federizon J; Rzayev J; Sukumaran DK; Alexandridis P; Lovell JF Therapeutic surfactant-stripped frozen micelles. Nat Commun 2016, 7, 11649. [PubMed: 27193558]

(42). Harris JM; Chess RB Effect of pegylation on pharmaceuticals. Nat Rev Drug Discov 2003, 2 (3), 214. [PubMed: 12612647]

(43). Lipka J; Semmler-Behnke M; Sperling RA; Wenk A; Takenaka S; Schleh C; Kissel T; Parak WJ; Kreyling WG Biodistribution of PEG-modified gold nanoparticles following intratracheal instillation and intravenous injection. Biomaterials 2010, 31 (25), 6574. [PubMed: 20542560]

(44). Vonarbourg A; Passirani C; Saulnier P; Benoit J-P Parameters influencing the stealthiness of colloidal drug delivery systems. Biomaterials 2006, 27 (24), 4356. [PubMed: 16650890]

(45). Xu M; Wang LV Universal back-projection algorithm for photoacoustic computed tomography. Phys. Rev. E 2005, 71 (1), 016706.

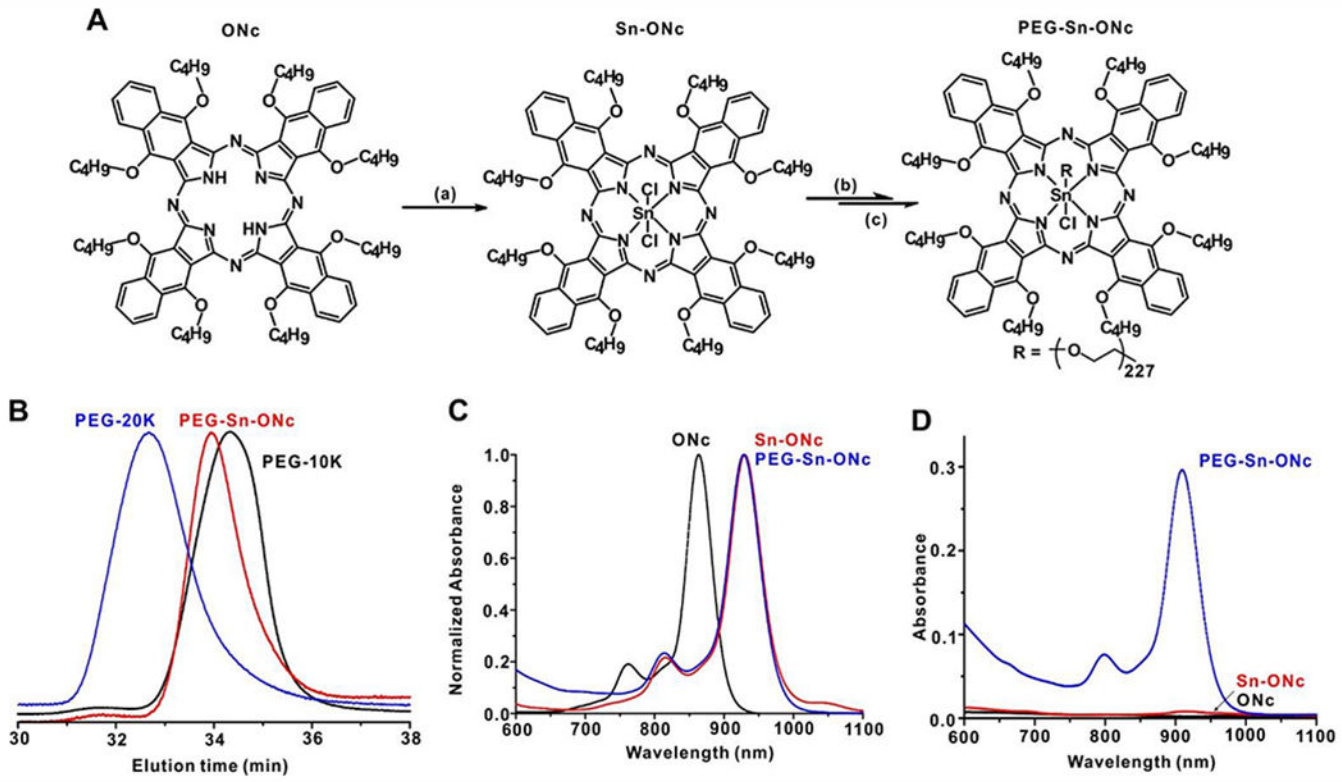

Figure 1.

Synthesis of PEG-Sn-ONc (A) Synthesis procedure. Conditions: (a) $SnCl_2 \cdot 2H2O$, DMF, 163 °C reflux, 4h; (b) $AgPF_6$, anhydrous toluene, 60 °C overnight; (c) PEG-10K and NaH, anhydrous toluene, refluxed 3h, and transferred to the $AgPF_6$-reacted Sn-ONc solution and refluxed for 48h. (B) Gel permeation chromatography of PEG-Sn-ONc (red), PEG-10K (10 kDa, black) and PEG-20K (20 kDa, blue). (C) Normalized absorbance spectra of ONc (black), Sn-ONc (red) and PEG-Sn-ONc (blue) in methylene chloride. (D) Absorbance of soluble fraction (supernatants) of dyes dissolved in methanol. ONc (black), Sn-ONc (red) and PEG-Sn-ONc (blue). Supernatants were diluted 100 times prior to measurement

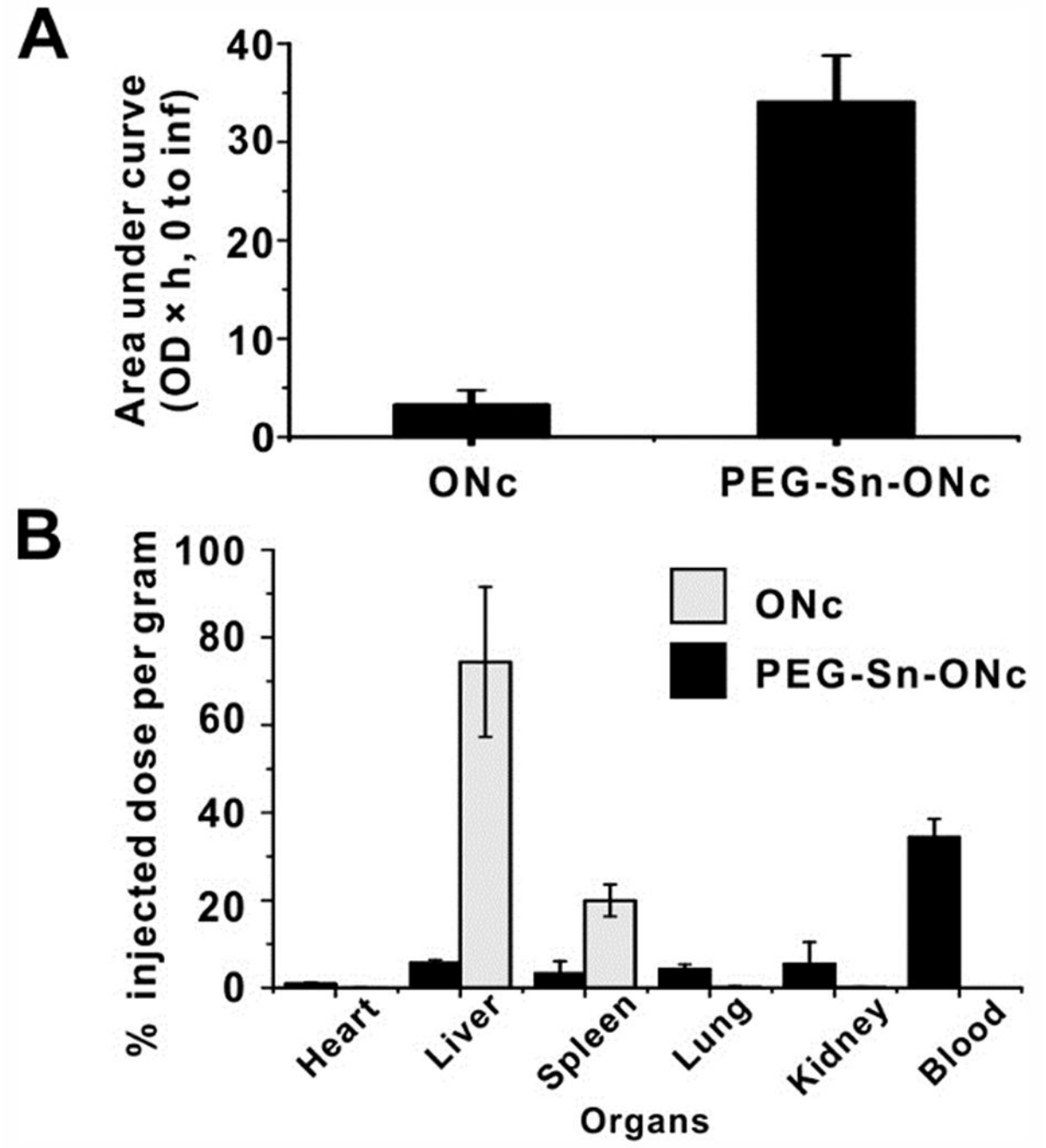

Figure 2.

(A) Area under the blood concentration-time curve of ONc and PEG-Sn-ONc. (B) Biodistribution of PEG-Sn-ONc (black) and ONc (grey) 24 hours after intravenous administration.

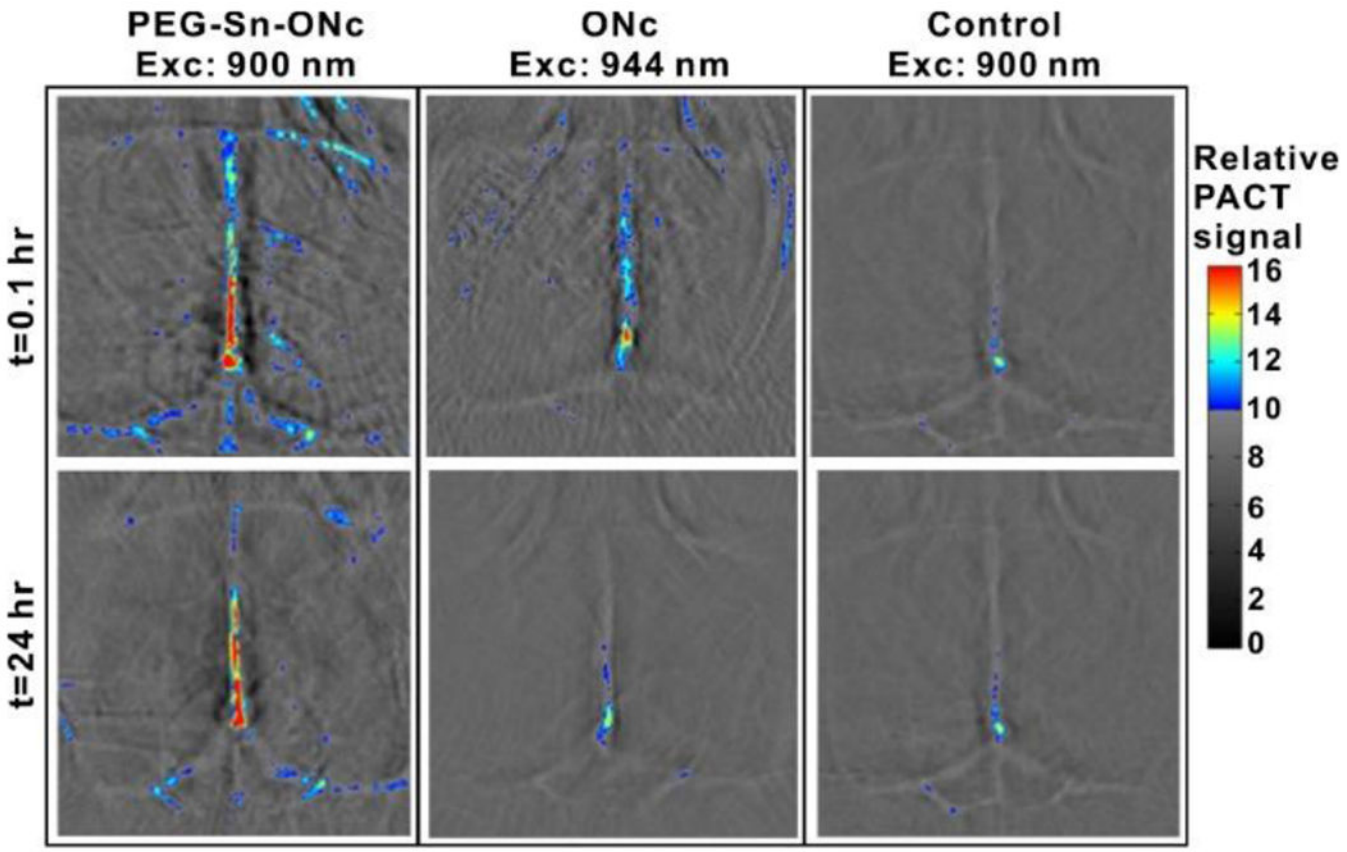

Figure 3.

Non-invasive photoacoustic images of brain blood vessels of mice administered with 6 O.D. of PEG-Sn-ONc or ONc at the indicated time points following intravenous injection.

Table 1.

Blood circulation parameters

	ONc	PEG-Sn-ONc
Injected Dose (O.D.)	6	6
$t_{1/2}$ (h)	1.7 ± 1.2	5.6 ± 1.2
Mean Residence Time (h)	2.5 ± 1.7	8.1 ± 1.8
Steady state volume of distribution (O.D./O.D)	4.2 ± 1.0	1.4 ± 0.25